Supporting information

Exploring the Compositional Space of a Metal-Organic Framework with Ionic Liquids to develop Porous Ionic Conductors for Enhanced Signal and Selectivity in VOC Capacitive Sensors

Bruna F. Gonçalves*[,1], Eduardo Fernández[1], Ainara Valverde[1], Mattia Gaboardi[2], Hugo Salazar[1], Viktor Petrenko[1,3], José María Porro[1,3], Leide P. Cavalcanti[4], Karmele Urtiaga[5], José M.S.S. Esperança[6], Daniela M. Correia[7], Felix Fernandez-Alonso[2,3,8], Senentxu Lanceros-Mendez[1,3], Roberto Fernández de Luis[1]

[1]BCMaterials, Basque Center for Materials, Applications and Nanostructures, UPV/EHU Science Park, 48940 Leioa, Spain

[2]Materials Physics Center, CSIC-UPV/EHU, Paseo Manuel de Lardizabal 5, 20018, Donostia - San Sebastian, Spain

[3]IKERBASQUE, Basque Foundation for Science, 48009 Bilbao, Spain

[4]ISIS Neutron and Muon Source, Science and Technology Facilities Council, Rutherford Appleton Laboratory, Didcot OX11 0QX, United Kingdom

[5]Geology Department, University of the Basque Country (UPV/EHU), Barrio Sarriena s/n, 48940, Leioa, Spain

[6]LAQV, REQUIMTE, Departamento de Química, Faculdade de Ciências e Tecnologia, Universidade Nova de Lisboa, 2829-516, Lisboa, Portugal

[7] Chemistry Centre of Minho and Porto Universities (CF-UM-UP), University of Minho, 4710-057, Braga, Portugal

[8]Donostia International Physics Center (DIPC), Paseo Manuel de Lardizabal 4, 20018 Donostia San Sebastian, Spain

[9]Physics Centre of Minho and Porto Universities (CF-UM-UP), University of Minho, 4710-057, Braga, Portugal

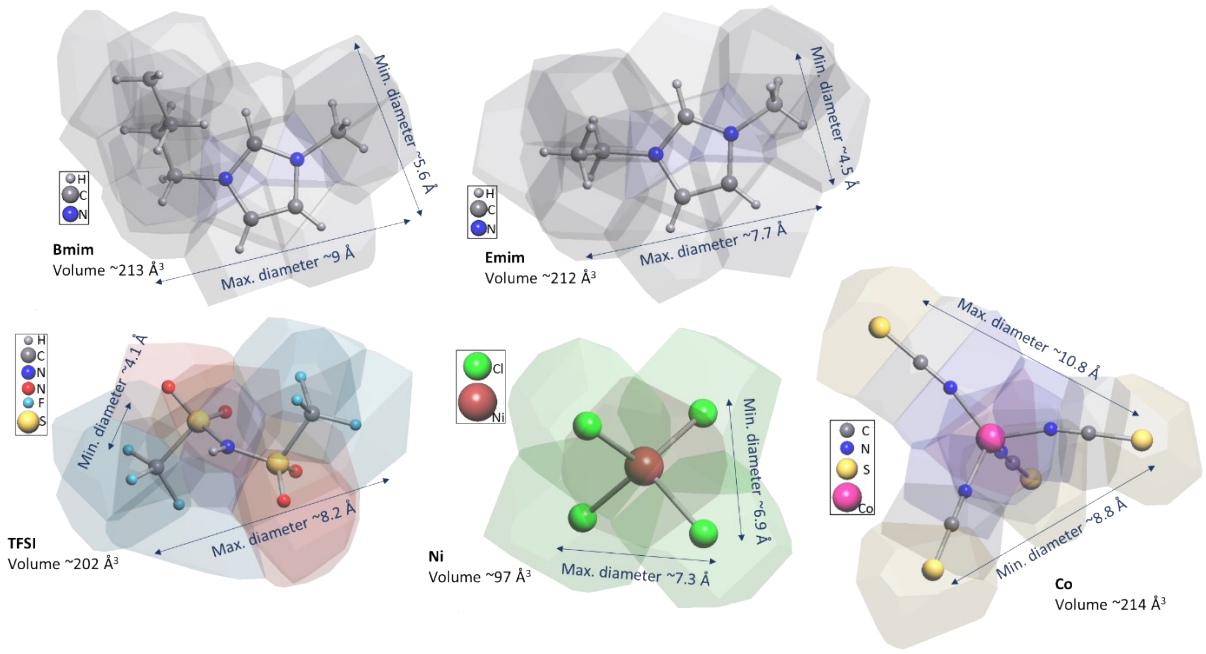

Figure S1. Cations and anions of the IL with the corresponding volume and minimum and maximum diameter.

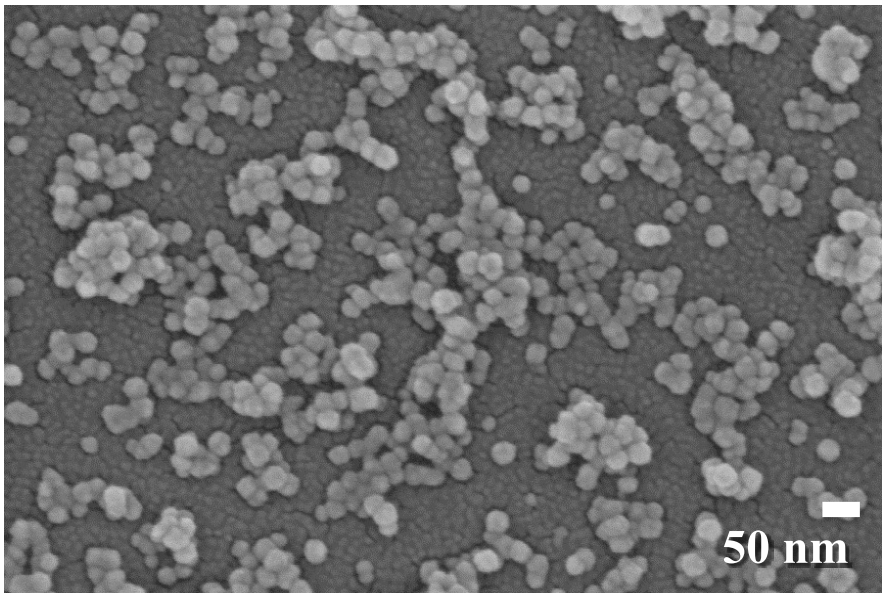

Figure S2. Scanning electron microscopy of the synthesized ZIF-8 nanoparticles.

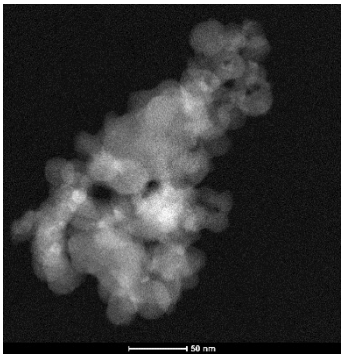

Figure S3. HAADF-STEM image of the synthesized ZIF-8 nanoparticles.

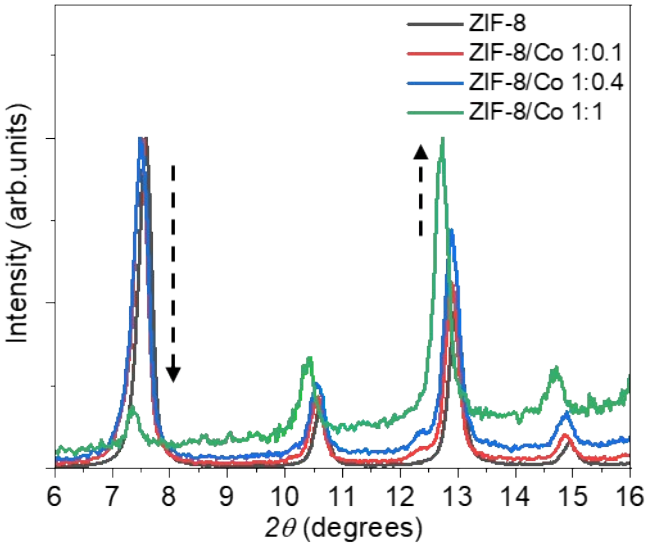

Figure S4. X-Ray diffraction patterns of neat ZIF-8 and ZIF-8/IL Co samples. The intensity increase/decrease trend is indicated by arrows.

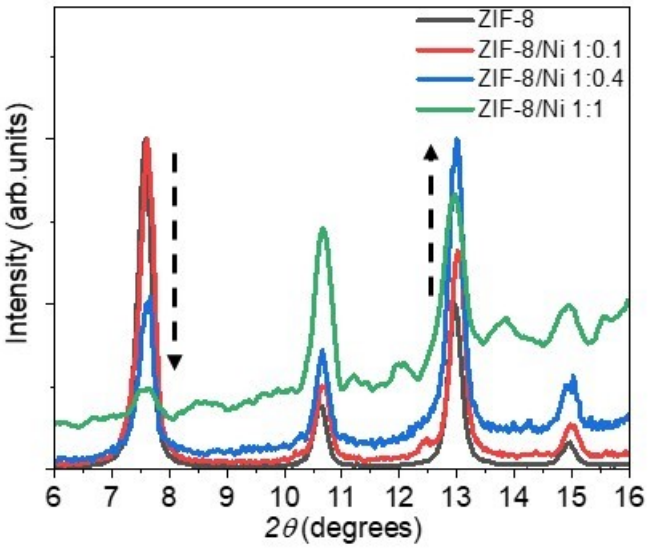

Figure S5. X-Ray diffraction patterns of neat ZIF-8 and ZIF-8/IL Ni samples. The intensity increase/decrease trend is indicated by arrows.

Table S1. Cell parameters obtained from the pattern matching fittings for ZIF-8/IL-Ni and ZIF-8/IL-Co samples.

Sample	Cell parameters (Å)
ZIF-8/IL-Ni (1:0.1)	17.0090
ZIF-8/IL-Ni (1:0.4)	17.0935
ZIF-8/IL-Ni (1:1)	17.1860
ZIF-8/IL-Co (1:0.1)	17.0381
ZIF-8/IL-Co (1:0.4)	17.0350
ZIF-8/IL-Co (1:1)	17.1450

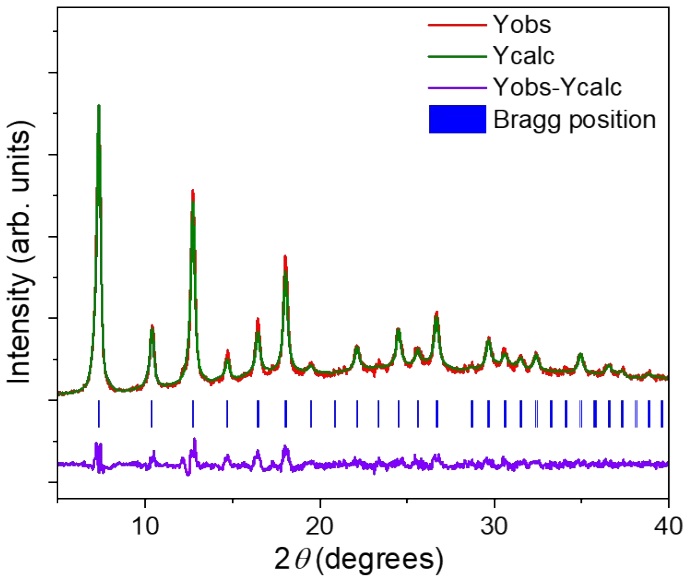

Figure S6. Fitting of the XRD patterns of ZIF-8/IL-Co 1:0.4 Chi^2=1.70 by a full profile matching.

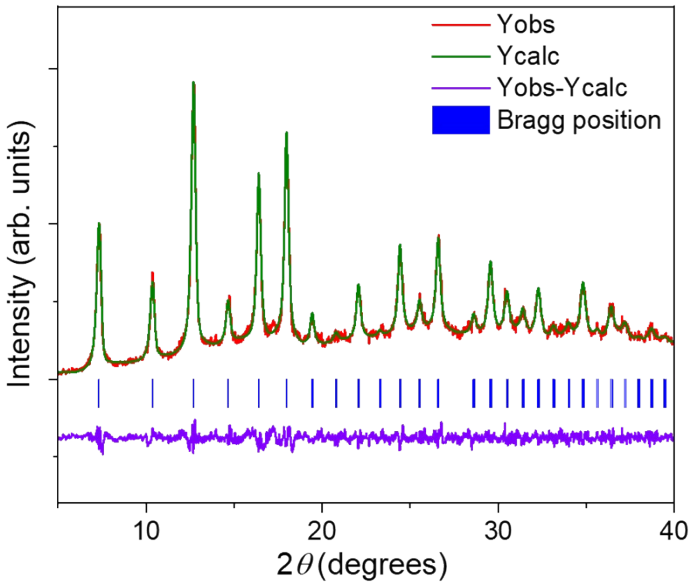

Figure S7. Fitting of the XRD patterns of ZIF-8/IL-Ni 1:0.4 Chi^2=0.96 by a full profile matching.

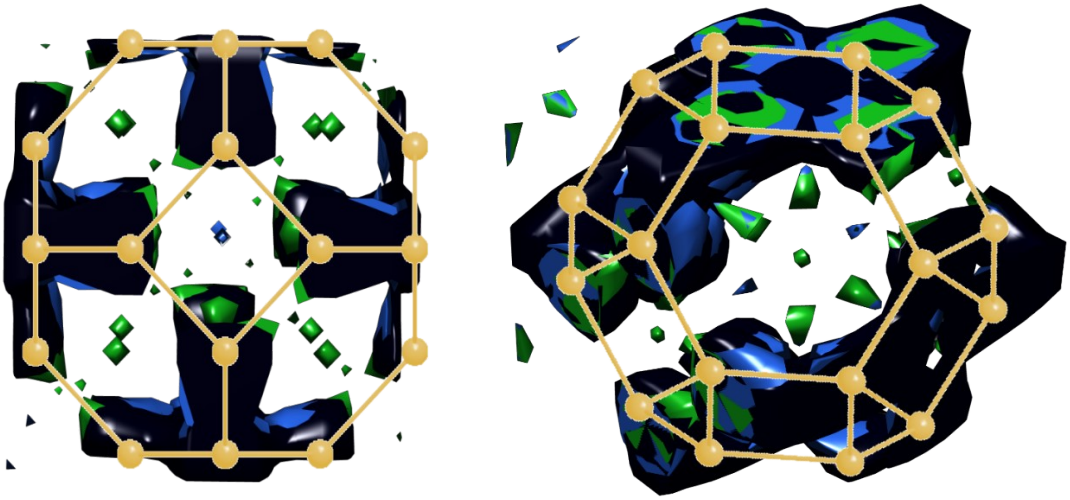

Figure S8. Difference envelope density simulations for ZIF-8 and ZIF-8/IL Co 1:0.4 and 1:1 samples. Black for ZIF-8, blue for ZIF-8/IL Co 1:0.4, green for ZIF-8/IL Co 1:1. The ZIF-8 chemical structure is represented in yellow.

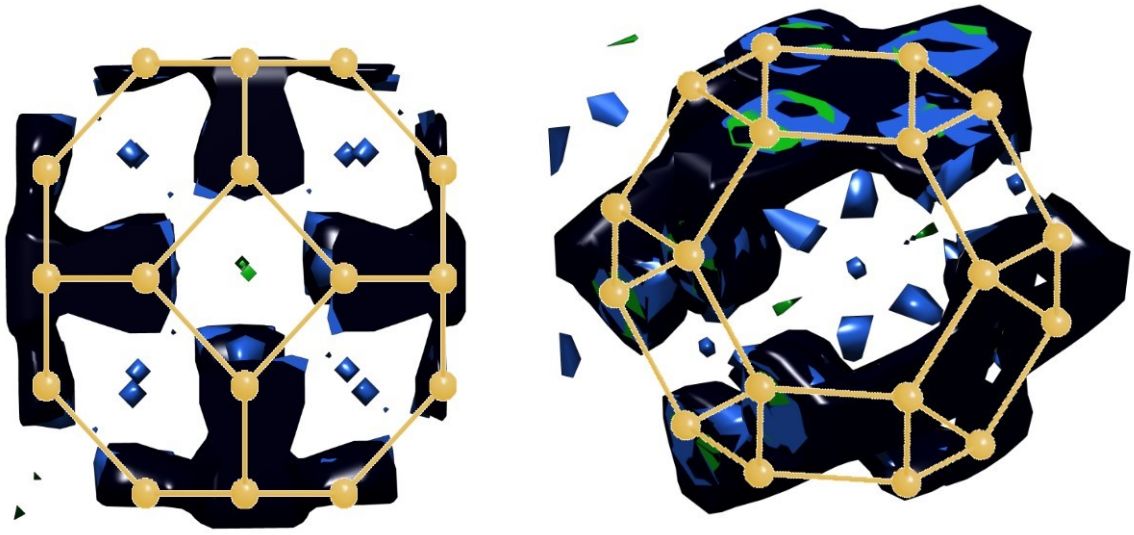

Figure S9. Difference envelope density simulations for ZIF-8 and ZIF-8/IL Ni 1:0.4 and 1:1 samples. Black for ZIF-8, blue for ZIF-8/IL Ni 1:0.4, green for ZIF-8/IL Ni 1:1. The ZIF-8 chemical structure is represented in yellow.

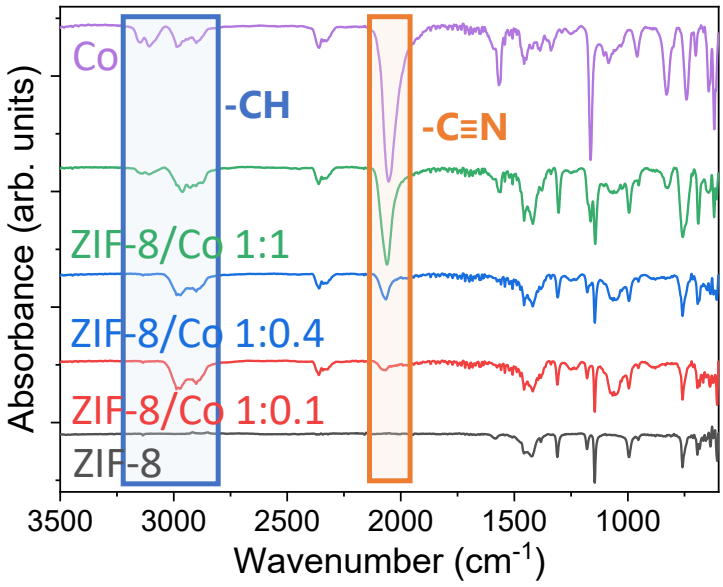

Figure S10. Fourier-transform infrared spectra of neat ZIF-8, ZIF-8/IL Co (1:0.1, 1:0.4 and 1:1), and neat IL Co samples.

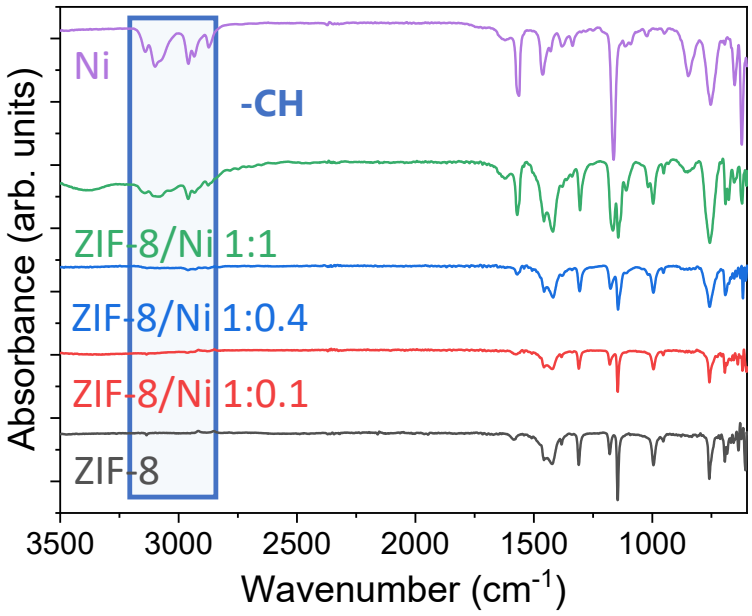

Figure S11. Fourier-transform infrared spectra of neat ZIF-8, ZIF-8/IL Ni (1:0.1, 1:0.4 and 1:1), and neat IL Ni samples.

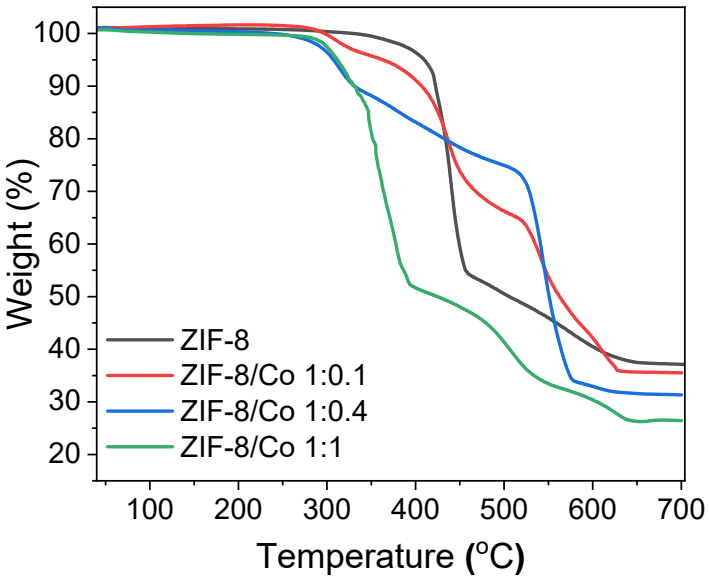

Figure S12. Thermogravimetric analysis curves of neat ZIF-8 and ZIF-8/IL Co (1:0.1, 1:0.4 and 1:1) samples.

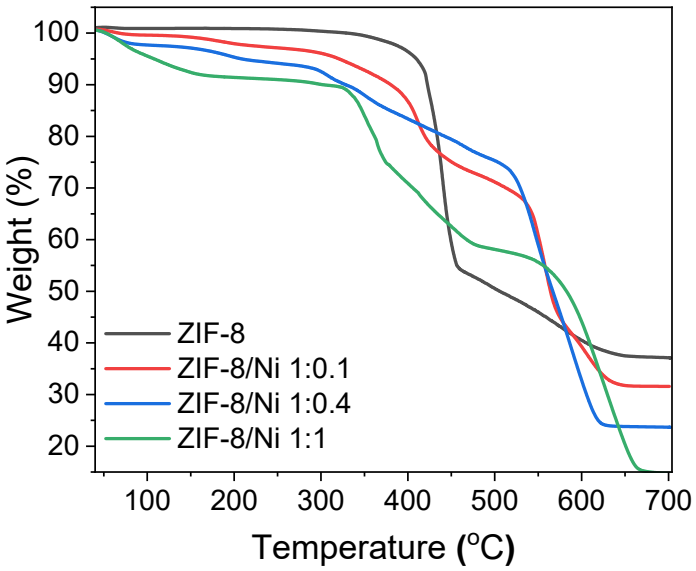

Figure S13. Thermogravimetric analysis curves of neat ZIF-8 and ZIF-8/IL Ni (1:0.1, 1:0.4 and 1:1) samples.

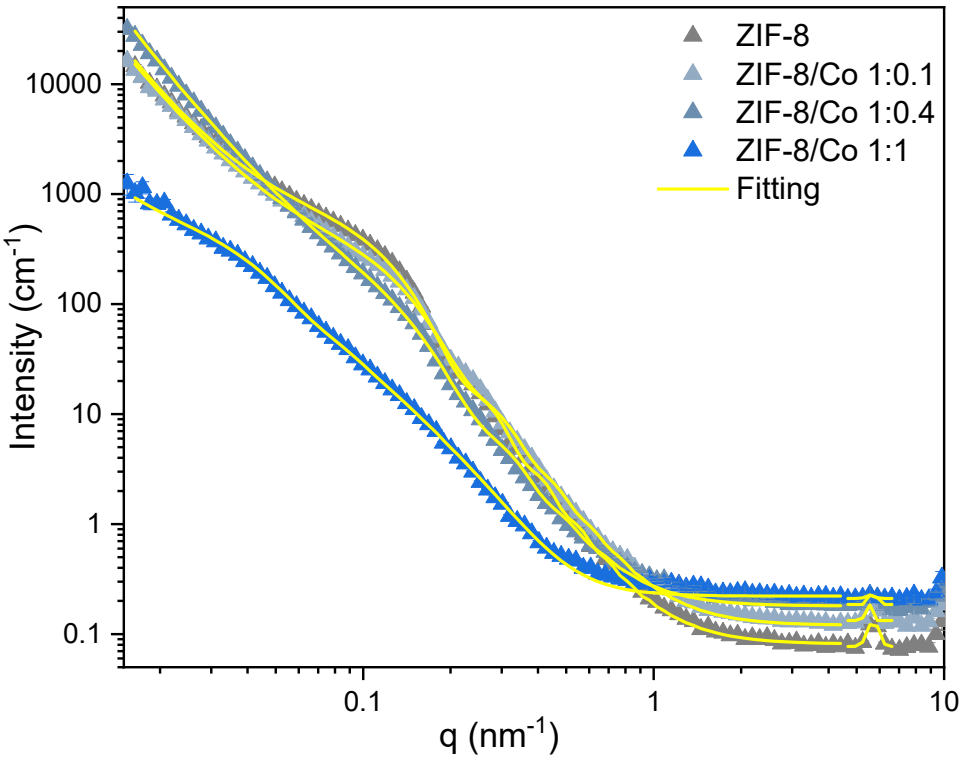

Figure S14. Small angle neutron scattering data of ZIF-8 and ZIF-8/Co (1:0.1, 1:0.4 and 1:1) composites with corresponding fitting.

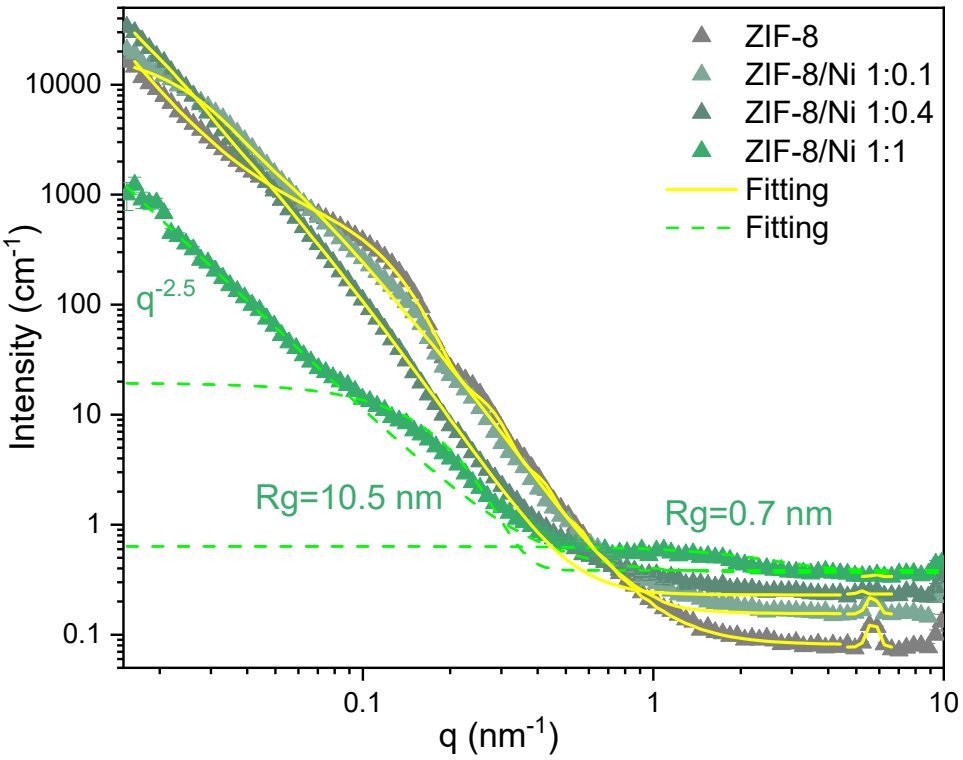

Figure S15. Small angle neutron scattering data of ZIF-8 and ZIF-8/Ni (1:0.1, 1:0.4 and 1:1) composites with corresponding fitting.

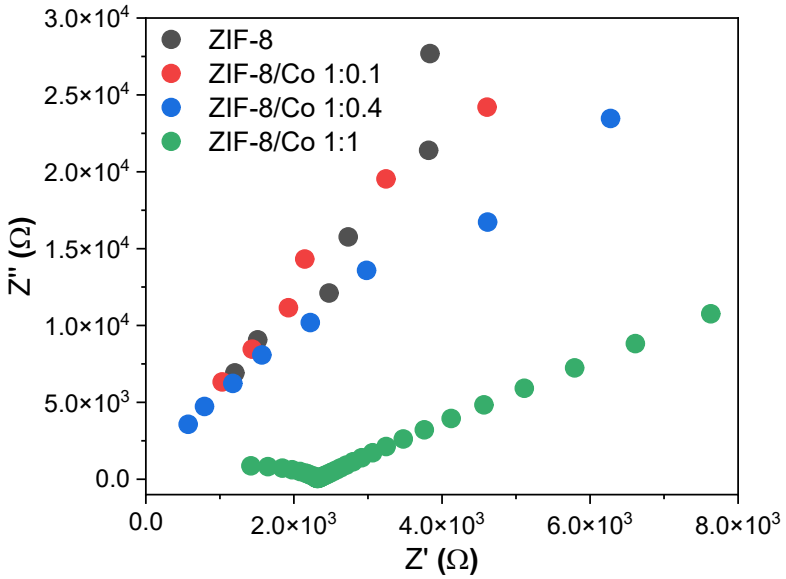

Figure S16. Nyquist plots of neat ZIF-8 and ZIF-8/IL Co (1:0.1, 1:0.4 and 1:1) samples.

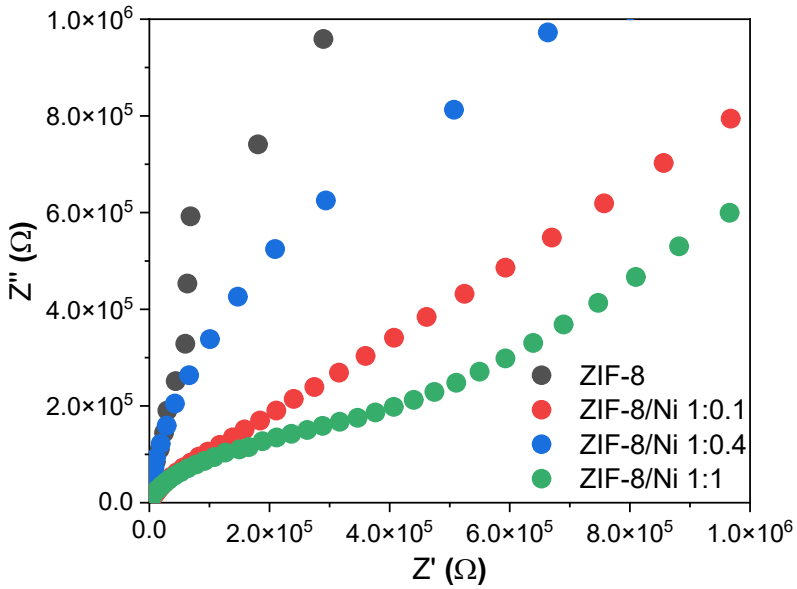

Figure S17. Nyquist plots of neat ZIF-8 and ZIF-8/IL Ni (1:0.1, 1:0.4 and 1:1) samples.

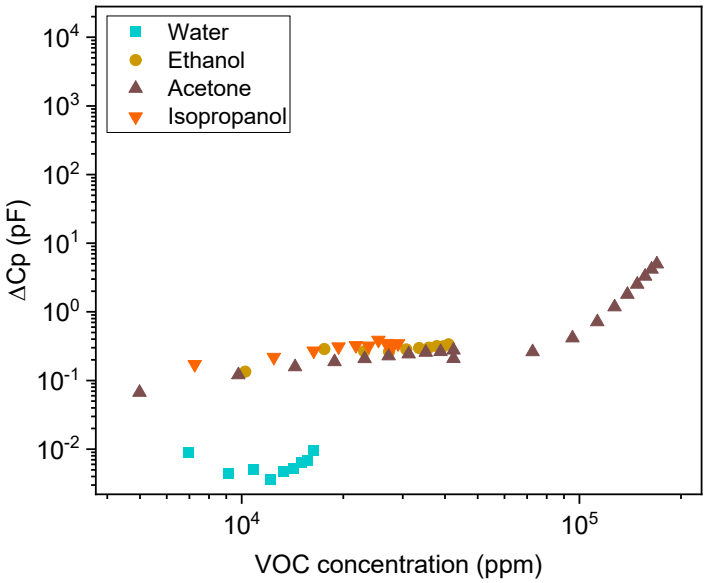

Figure S18. ΔCp vs VOC concentration data for IPA, acetone, ethanol, and water vapour for ZIF-8/Co 1:0.4.

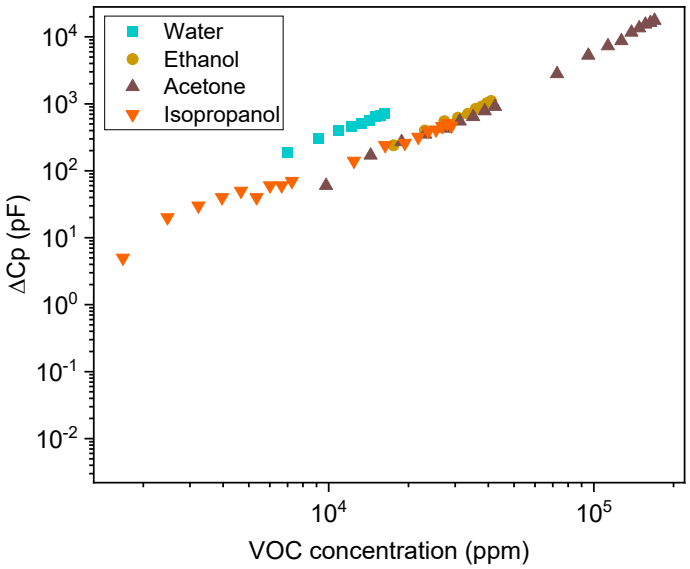

Figure S19. ΔCp vs VOC concentration data for IPA, acetone, ethanol, and water vapour for IL Co.

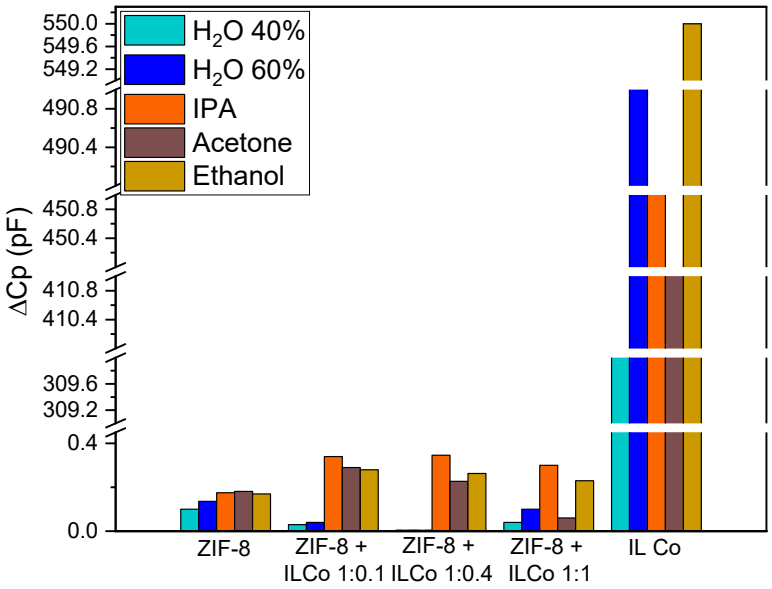

Figure S20. Bar chart with ΔCp for neat ZIF-8, ZIF-8/Co (1:0.1, 1:0.4, and 1:1), and IL Co for 40 and 60% relative humidity, IPA, acetone, ethanol, and water.

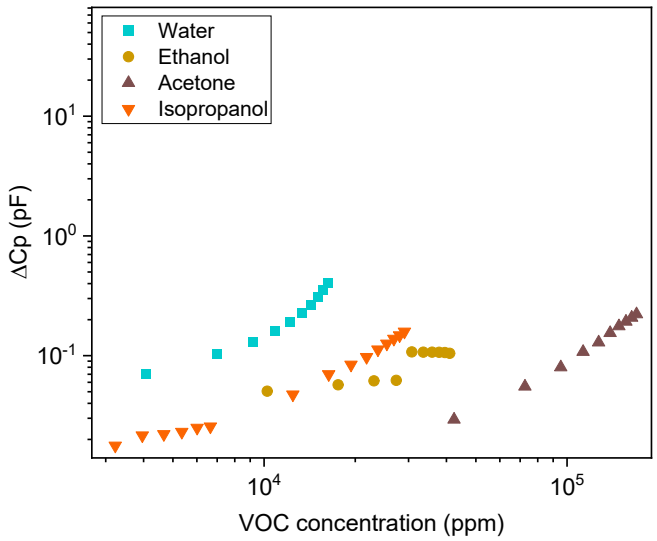

Figure S21. ΔCp vs VOC concentration data for IPA, acetone, ethanol, and water vapour for ZIF-8/Ni 1:0.4.

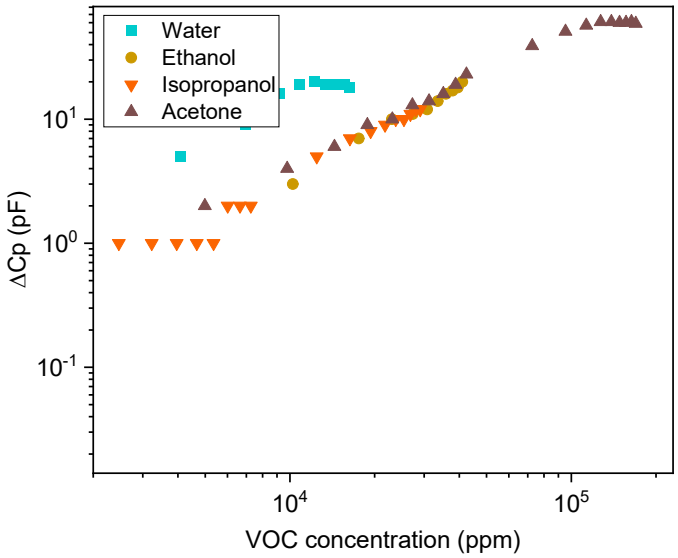

Figure S22. ΔCp vs VOC concentration data for IPA, acetone, ethanol, and water vapour for IL Ni.

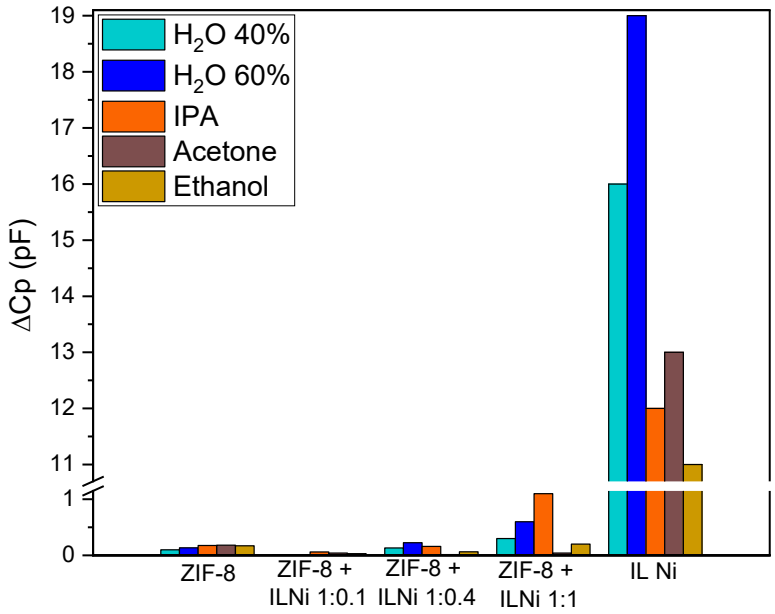

Figure S23. Bar chart with ΔCp for neat ZIF-8, ZIF-8/Ni (1:0.1, 1:0.4, and 1:1), and IL Ni for 40 and 60% relative humidity, IPA, acetone, ethanol, and water.

Table S2. Sensors evaluation in means of LoD and sensitivity towards each vapour (water, ethanol, IPA, and acetone).

Sample	Vapour	LoD (ppm)	Sensitivity (pF/ppm)	Sensitivity* (pF/ppm)
ZIF-8/TFSI 1:0.1	Water	16048	$1.3x10^{-5}$	---
	Ethanol	7151	$7.0x10^{-5}$	---
	IPA	8080	$6.0x10^{-5}$	---
	Acetone	9842	$2.4x10^{-5}$	$7.4x10^{-4}$
ZIF-8/TFSI 1:1	Water	6841	$2.4x10^{-6}$	---
	Ethanol	4476	$2.4x10^{-6}$	$8.2x10^{-6}$
	IPA	4042	$4.9x10^{-6}$	---
	Acetone	6886	$3.1x10^{-6}$	$2.2x10^{-4}$
IL Co	Water	3424	$4.6x10^{-2}$	---
	Ethanol	11598	$2.7x10^{-2}$	---
	IPA	4930	$1.8x10^{-2}$	---
	Acetone	9554	$2.2x10^{-2}$	$1.6x10^{-1}$
ZIF-8/Co 1:0.1	Water	17984	$2.6x10^{-6}$	---
	Ethanol	16167	$1.9x10^{-5}$	
	IPA	11368	$1.3x10^{-5}$	
	Acetone	109214	$5.3x10^{-6}$	

ZIF-8/Co 1:0.4	Water	9282	$4.6x10^{-7}$	---
	Ethanol	11955	$7.5x10^{-6}$	---
	IPA	11728	$1.1x10^{-5}$	---
	Acetone	13558	$6.1x10^{-6}$	$8.9x10^{-5}$
ZIF-8/Co 1:1	Water	6240	$7.5x10^{-6}$	---
	Ethanol	18297	$7.6x10^{-6}$	$4.2x10^{-5}$
	IPA	6951	$2.6x10^{-6}$	$2.1x10^{-5}$
	Acetone	9545	$2.8x10^{-6}$	$1.6x10^{-3}$
IL Ni	Water	7089	$1.2x10^{-3}$	---
	Ethanol	6660	$4.8x10^{-4}$	
	IPA	3012	$4.4x10^{-4}$	
	Acetone	10718	$5.1x10^{-4}$	
ZIF-8/Ni 1:0.1	Water	10925	$8.9x10^{-7}$	---
	Ethanol	17660	$1.4x10^{-6}$	
	IPA	30516	$1.6x10^{-6}$	
	Acetone	45433	$5.8x10^{-7}$	
ZIF-8/Ni 1:0.4	Water	1480	$1.5x10^{-5}$	$6.0x10^{-5}$
	Ethanol	15507	$2.6x10^{-6}$	---
	IPA	4883	$5.2x10^{-6}$	---
	Acetone	16693	$8.3x10^{-7}$	$2.1x10^{-6}$
ZIF-8/Ni 1:1	Water	5202	$4.6x10^{-5}$	$4.6x10^{-4}$
	Ethanol	14914	$6.8x10^{-6}$	---
	IPA	10615	$1.2x10^{-5}$	$2.2x10^{-4}$
	Acetone	41738	$1.0x10^{-6}$	---

* in the case of samples with two different linear regressions (one at low [VOC] and one at high [VOC]).